IL NUOVO CIMENTO Vol. 33 C, N. 2 Marzo-Aprile 2010
DOI 10.1393/ncc/i2010-10610-5

Colloquia: LC09

Physical problems for future Photon Colliders

I. F. Ginzburg

Sobolev Institute of Mathematics and Novosibirk State University - Novosibirsk, Russia

(ricevuto il 20 Febbraio 2010; approvato il 30 Marzo 2010; pubblicato online il 7 Luglio 2010)

Summary. — In this report I discuss physical problems for future Photon Colliders (PLC), which can be stated AFTER 10 years of work of LHC and few years of work of e^+e^- ILC. I discuss mainly the unfavorable case when these colliders will give us only Higgs boson(s) and perhaps some charged particles of unclear nature. I focus my attention on the case of PLC based on the second stage of ILC (about 1 TeV) or CLIC (1–3 TeV). It offers the opportunity to study new series of fundamental physical problems. Among them, multiple production of gauge bosons, hunt for strong interaction in Higgs sector, search of exotic interactions in the process $\gamma\gamma \to \gamma\gamma$ with final photons having transverse momenta ~ 0.5–$0.7E_e$.

PACS 29.20.Ej – Linear accelerators.
PACS 13.66.Lm – Processes in other lepton-lepton interactions.
PACS 14.70.-e – Gauge bosons.
PACS 14.80.-j – Other particles (including hypothetical).

1. – Introduction. Different opportunities for PLC

We discuss here Photon Colliders (PLC) for different energy ranges. To do that, we start with repetition of the basic scheme (see fig. 1) [1]. The focused laser flash meets the electron bunch of LC in the *conversion point C* at a small distance b before the *interaction point IP*. In C a laser photon scatters on a high-energy electron taking from it a large portion of energy. Scattered photons travel along the direction of the initial electron with angular spread $\sim 1/\gamma_e \equiv m_e c^2/E$, they are focused in the IP. Here they collide with an opposite electron ($e\gamma$ collider) or a photon ($\gamma\gamma$ collider).

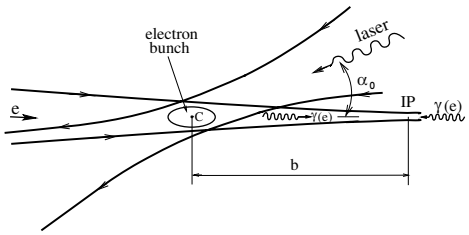

Fig. 1. – Photon Collider. Basic scheme.

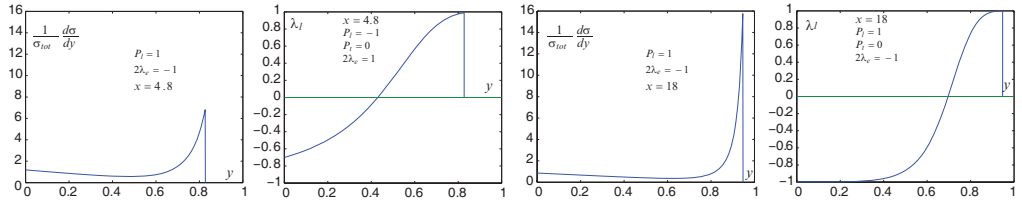

Fig. 2. – Photon energy and polarization spectra, left $x = 4.8$, right $x = 18$.

For the ILC-1 based PLC, the laser flash with energy of a few Joules and length of a few mm is sufficient. The preferable form of basic electron beam for PLC is different from that for e^+e^- LC. Based on that one can make the $\gamma\gamma$ luminosity of PLC even larger than that of basic e^+e^- LC. In known projects this opportunity is used only weakly. *The total additional cost is estimated in this case as* $\sim 10\%$ *from that of LC* [2].

The energy spectrum of the obtained photon beam is concentrated near its upper bound. If E_e is the electron energy and $x = 4E_e\omega_0/(m^2c^4)$, then $E_{\gamma,\max} = E_e x/(x+1)$. Spectrum becomes sharper with a suitable choice of polarizations of initial electrons and laser photons and with growth of x. The obtained photon beam is strongly polarized. The photon energy and mean photon helicity spectra are presented in fig. 2 in dependence on $y = \omega/E_e$ for the case when initial electron helicity $\lambda_e = -1/2$ and initial laser photons are right polarized (helicity $P_l = 1$) for two values of x.

The real picture is more complex.

i) When photons with energy $\omega < \omega_{\max}$ propagate from the collision point C to the interaction point IP, they distribute over a wider area reducing $\gamma\gamma$ luminosity in its soft part.

ii) The low-energy part of spectra is increased due to multiple rescatterings of electrons on the other laser photons.

iii) The nonlinear QED effects also modify spectra, mainly for the case $x \leq 4.8$.

iv) At $x > 4.8$ some fractions of produced photons disappear in the collision with laser photon, $\gamma\gamma_0 \to e^+e^-$. This effect results in strong limitation for the practical conversion coefficient.

In future practice, the luminosity/polarization spectra should be measured during operations simultaneously with new physical data.

The production of photon beam for the LC with the electron energy $E_e > 250\,\mathrm{GeV}$ causes difficult problems making construction of PLC for this energy range doubtful [3]. We consider here briefly two main ways of production of photon beams for $E_e \sim 1\,\mathrm{TeV}$ [4].

The first way is to use the conversion scheme [1] with infrared or free electron laser to reach the highest luminosity. The laser photon energy ω_0 will be 0.5–0.2 eV with $x = 4.8$ which prevents e^+e^- pair production in collision of high energy and laser photons. To get high conversion coefficient, the conversion process has to take place with large non-linear QED effects, making final photon distributions less monochromatic and less polarized. Here one must work with infrared optics which causes additional difficulties (see discussion in [3]).

TABLE I. – *Parameters of PLC for two ways.*

	Way →	I, $x = 4.8$	II, $x = 18$
A	Necessary laser flash energy (J)	< 5	< 5
B	The conversion coefficient $e \to \gamma$	0.7	0.15
C	Maximal photon energy $E_{\gamma\,\max}$	$0.8E_e$	$0.95E_e$
D	Luminosity $\mathcal{L}_{\gamma\gamma}/\mathcal{L}_{e^+e^-}$	0.35	0.03–0.05
E	Luminosity $\mathcal{L}_{e\gamma}/\mathcal{L}_{e^+e^-}$	0.25	0.2
F	Mean energy spread $\langle\Delta E_\gamma\rangle$	$0.07E_{\gamma\,\max}$	$0.03E_{\gamma\,\max}$
G	Mean photon helicity $\langle\lambda_\gamma\rangle$	0.95	0.95

The second way is to use the same laser (and the same optics) as for the electron beam energy 250 GeV (ILC-1)—with photon energy $\omega_0 \sim 1$ eV—but we limit ourselves by a small conversion coefficient $k \leq 0.14$ (at $x = 18$) [4]. This value assures that the losses of high-energy photons due to e^+e^- pair production in collision of high-energy photon with laser photon are small. At this value of conversion coefficient the non-linear QED effects are insignificant and the contribution from rescatterings is small. Here the maximum photon energy is higher than in the first way, $\omega_m \approx (0.9\text{–}0.95)E$, energy distribution of high energy photons is sharper, etc., fig. 2, right. These advantages allow to consider this option despite the reduction of $\gamma\gamma$ luminosity by about one order in comparison with the first way. *The second way seems more attractive to me.*

The typical expected parameters of PLC for these two ways are presented in table I. Here lines D-G describe only the high-energy peak ($E_{\gamma 1,2} > 0.7E_{\gamma\,\max}$), which is separated well from the low-energy part of spectrum and luminosity, it depends only weakly on the details of the conversion scheme. In both schemes one can hope to have an annual luminosity 50–250 fb^{-1}/year.

The set of problems for PLC at ILC1 is widely discussed (see, *e.g.*, [2]). The study of some of them (with increase of thresholds for search of new particles) will be a natural task for PLC with higher beam energy. We select here problems to answer for questions: *what new can be studied at PLC AFTER about 10 years of work of LHC with higher beam energy, and perhaps, few years of work of e^+e^- ILC with slightly larger beam energy and luminosity.*

2. – QCD and hadron physics

The photon structure function is a unique object of QCD, calculable at large enough Q^2 without additional phenomenological parameters [5]. It can be measured at PLC in $e\gamma$ mode with high accuracy, since photon target with its energy and polarization here is practically known. The manipulation with beam polarizations will be an important instrument here.

The region of electron transverse momenta above 50 GeV ($M_Z/2$) can be studied well, providing the opportunity to study the effect of Z-boson exchange and $\gamma^* - Z$ interference.

The other studies like those at HERA are possible here.

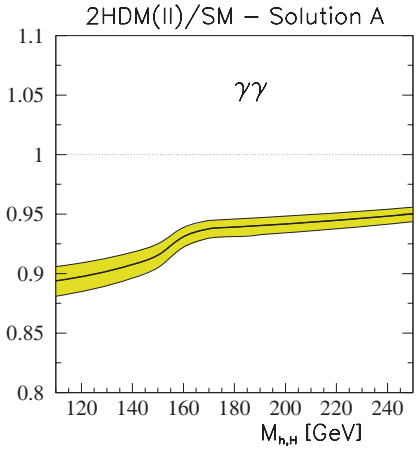

Fig. 3. – The ratio of $\Gamma(h \to \gamma\gamma)$ to its SM value for a typical class of realizations of SM-like scenario.

3. – Higgs physics

The Higgs mechanism of EWSB can be realized either by minimal Higgs sector with one observable neutral scalar Higgs boson (SM) or by non-minimal Higgs sector with a larger number of observable scalars. In this section for definiteness we consider SM and specific non-minimal Higgs sector—Two Higgs Doublet Model (2HDM). The latter is the simplest extension of Higgs sector of SM. It contains 2 complex Higgs doublet fields ϕ_1 and ϕ_2 with v.e.v.'s $v\cos\beta$ and $v\sin\beta$. The physical sector contains charged scalars $H^\pm$ and three neutral scalars h_i, generally having no definite CP parity. In the CP-conserving case these three h_i become two scalars h, H ($M_h < M_H$) and a pseudoscalar A. For definiteness, we assume the Model II for the Yukawa coupling in 2HDM (the same is realized in MSSM).

3˙1. *SM-like scenario. Distinguishing models.* – Let earlier observations discover Higgs boson, similar to that in SM (*SM-like scenario*). How to state whether we deal with SM Higgs boson or some other realization of Higgs sector (*e.g.*, 2HDM)? What can we say about properties of this realization?

LHC can measure Higgs couplings to particles only with low precision, typically 10–20%. The e^+e^- LC will improve these results up to 5–10%, sometimes better. The PLC can improve these accuracies further to about 1%. Here, measuring the $h\gamma\gamma$ ($hZ\gamma$) couplings is very promising. The expected accuracy in the measurement of the two-photon width is 2% at $M_h \leq 150\,\mathrm{GeV}$ and $\int \mathcal{L}dt = 30\,\mathrm{fb}^{-1}$ (by 5 times lower than the anticipated annual luminosity) [6].

Example—distinguishing SM/2HDM. The SM-like scenario means that the coupling constants *squared*, measured at LHC and e^+e^- LC, are *close* to the SM value within anticipated precision (not coupling constants themselves!) In the 2HDM this scenario can be realized in many ways.

The models can be distinguished via measurement of the $\gamma\gamma$ width of the observed SM-like Higgs boson, fig. 3 [7]. In this figure we show the ratio of $\Gamma(h \to \gamma\gamma)$ to its SM value for one typical class of realizations of SM-like scenario. The band reflects

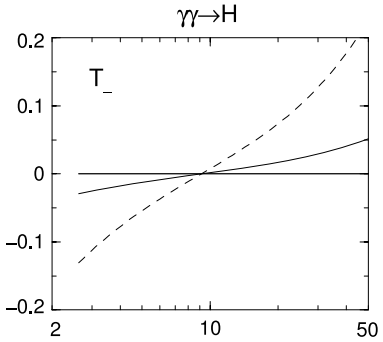

Fig. 4. – Effect of CP violation in 2HDM.

the anticipated uncertainty of future measurements. The deviation from SM, given by contributions of heavy charged Higgs bosons for a natural set of parameters, is about 10% (compare with the anticipated 2% accuracy). For the other sets of parameters, consistent with SM-like scenario, the deviation from SM is even larger.

3˙2. *CP violation in Higgs sector*. – In many extensions of Higgs model (*e.g.*, in 2HDM) observable neutral Higgs bosons h_i have generally *no* definite CP-parity and effectively

$$\mathcal{L}_{\gamma\gamma H} = G_\gamma^{\rm SM}\left[g_\gamma H F^{\mu\nu}F_{\mu\nu} + i\tilde{g}_\gamma H F^{\mu\nu}\tilde{F}_{\mu\nu}\right]; \quad g_\gamma \sim \tilde{g}_\gamma \sim 1. \tag{1}$$

Here $F^{\mu\nu}$ and $\tilde{F}^{\mu\nu} = \varepsilon^{\mu\nu\alpha\beta}F_{\alpha\beta}/2$ are the standard field strengths for the electromagnetic field. The relative effective couplings g and $\tilde{g}$ are described with the standard triangle diagram $H\gamma\gamma$, they are expressed with known equations via masses of charged fermions and W, and mixing parameters (parameters of 2HDM potential). They are generally complex ($b\bar{b}$-loop).

Total production cross section varies strongly with variation of circular λ_i and linear ℓ_i polarizations of photon beams and the angle ψ between linear polarization vectors [8]:

$$\begin{aligned}\sigma(\gamma\gamma\to H) = \sigma_{\rm np}^{\rm SM}\times\big[&|g_\gamma|^2(1+\lambda_1\lambda_2+\ell_1\ell_2\cos 2\psi)+|\tilde{g}_\gamma|^2(1+\lambda_1\lambda_2-\ell_1\ell_2\cos 2\psi)+\\ &+2\,\mathrm{Re}(g_\gamma^*\tilde{g}_\gamma)(\lambda_1+\lambda_2)+2\,\mathrm{Im}(g_\gamma^*\tilde{g}_\gamma)\ell_1\ell_2\sin 2\psi\big]\,.\end{aligned} \tag{2}$$

In particular, violation of CP symmetry in the Higgs sector leads to difference in the $\gamma\gamma\to H$ production cross sections in the collision of photons with identical total helicity (0) but with opposite helicities of separate photons:

$$T_- = \frac{\sigma(\lambda_i)-\sigma(-\lambda_i)}{\sigma_{\rm np}^{\rm SM}} \propto (\lambda_1+\lambda_2)\,\mathrm{Re}(g_\gamma\tilde{g}_\gamma^*). \tag{3}$$

Standard calculation of vertexes in the 2HDM at different parameters of model gives a typical dependence, shown in fig. 4 at $\lambda_1 = \lambda_2 = \pm 1$. It is seen that the effect is strong and can be measured well.

3˙3. *Observation of strong interaction in Higgs sector in $e\gamma \to eWW$ process at not too high energy.* – At high values of Higgs boson self-coupling constant, the Higgs mechanism of Electroweak Symmetry Breaking in Standard Model (SM) can be realized without actual Higgs boson but with strong interaction in Higgs sector (SIHS) which will manifest itself as a strong interaction of longitudinal components of W and Z bosons. It is expected that this interaction will be seen in the form of W_LW_l, W_LZ_L and Z_LZ_L resonances at 1.5–2 TeV. Main efforts to discover this opportunity are directed towards the observation of such resonant states. It is a difficult task for the LHC due to high background and it cannot be realized at the energies reachable at the ILC in its initial stages.

This strong interaction can be observed in the study of the charge asymmetry of produced $W^\pm$ in the process $e^-\gamma \to e^-W^+W^-$ similar to what was discussed in low-energy pion physics [9, 10]. To explain the set-up of the problem we discuss this process in SM [11].

We subdivide the diagrams of the process into three groups, where subprocesses of main interest are shown in boxes, sign $\otimes$ represents next stage of process.

a) Diagrams $e^- \to e^-\gamma^*(Z^*) \otimes \boxed{\gamma\gamma^*(\gamma Z^*) \to W^+W^-}$ contain subprocesses $\gamma\gamma^* \to W^+W^-$ and $\gamma Z^* \to W^+W^-$, modified by the strong interaction in the Higgs sector (*two-gauge*).

b) Diagrams $\gamma e^- \to e^{-*} \to e^-\gamma^*(Z^*) \otimes \boxed{\gamma^*(Z^*) \to W^+W^-}$ contain subprocesses $\gamma^* \to W^+W^-$ and $Z^* \to W^+W^-$, modified by the strong interaction in the Higgs sector (*one-gauge*).

c) Diagrams $\gamma \oplus \boxed{e^- \to W^-W^+e^-}$ are prepared by connecting the photon line to each charged particle line to the diagram shown inside the box. Strong interaction does not modify this contribution. These contributions are switched off at suitable electron polarization.

The subprocess $\gamma\gamma^* \to W^+W^-$ (from contribution a)) produces C-even system W^+W^-, the subprocess $\gamma^* \to W^+W^-$ (from contribution b)) produces C-odd system W^+W^-. The interference of similar contributions for the production of pions is responsible for large enough charge asymmetry, very sensitive to the phase difference of S (D) and P waves in $\pi\pi$ scattering [9]. This very phenomenon also takes place in the discussed case of W's. However, for the production of $W^\pm$ subprocesses with the replacement of $\gamma^* \to Z^*$ are also essential. Therefore, the final states of each type have no definite C-parity. Hence, charge asymmetry appears both due to interference between contributions of types a) and b) and due to interference of γ^* and Z^* contributions each within their own types.

3˙4. *Asymmetries in SM.* – To observe the main features of the effect of charge asymmetry and its potential for the study of strong interaction in the Higgs sector, we calculated some quantities describing charge asymmetry for $e^-\gamma$ collision at $\sqrt{s} =$ 500 GeV with polarized photons. We used CalcHEP package [12] for simulation.

We denote by $p^\pm$ momenta of $W^\pm$, by p_e-momentum of the scattered electron and $w = \frac{\sqrt{(p^+ + p^-)^2}}{2M_W}$, $v_1 = \frac{\langle (p^+ - p^-)p_e\rangle}{\langle (p^+ + p^-)p_e\rangle}$. We present below the dependence of the charge asymmetric quantity v_1 on w. The w-dependences for the other charge asymmetric quantities have similar qualitative features [11].

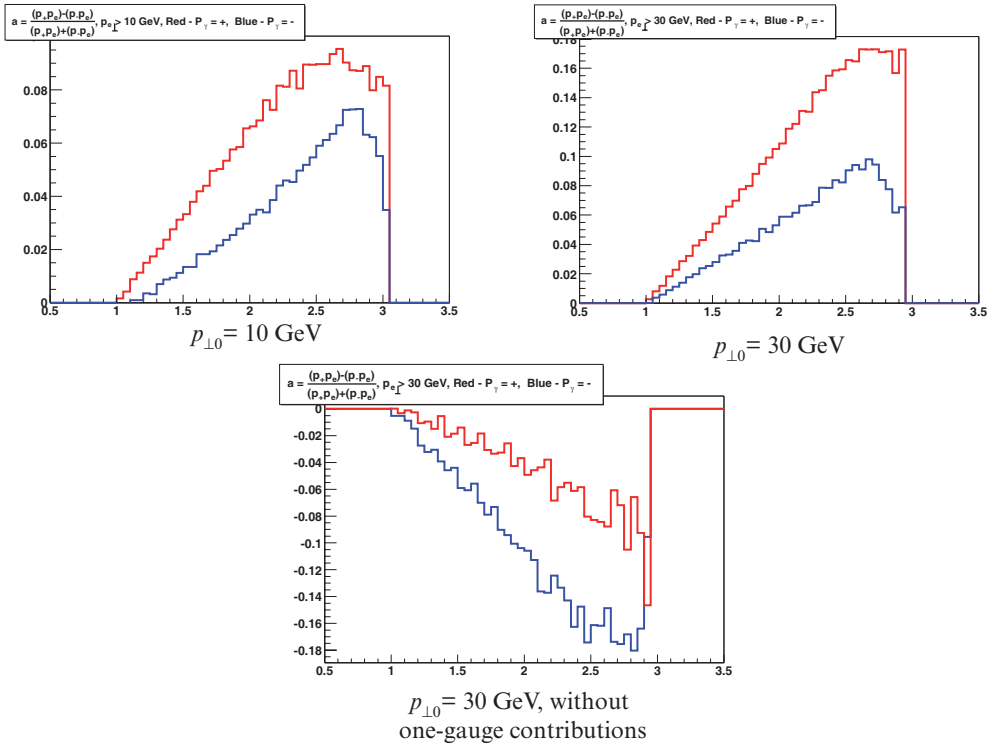

Fig. 5. – Distribution of v_1 in dependence on w. The upper curves are for right-handed polarized photons, the lower curves are for left-handed polarized photons.

We applied *the cut in transverse momentum of the scattered electron*,

$$p_\perp^e \geq p_{\perp 0} \qquad \text{with} \qquad \text{a)} \;\; p_{\perp 0} = 10\,\text{GeV}, \quad \text{b)} \;\; p_{\perp 0} = 30\,\text{GeV}. \tag{4}$$

Observation of the scattered electron allows to check kinematics completely.

Influence of polarization. Figure 5 (upper plots) represents the distribution in variable v_1 on photon polarization and cut in $p_\perp^e$. We did not study the dependence on electron polarization. This dependence is expected to be weak in SM where the main contribution to cross section is given by diagrams of type a) with virtual photons having the lowest possible energy. These photons "forget" the polarization of the incident electron. The strong-interaction contribution becomes essential at highest effective masses of the WW system with high energy of the virtual photon or Z, the helicity of which reproduces almost completely the helicity of the incident electron [13]. The study of this dependence will be a necessary part of studies beyond SM.

Significance of different contributions. To understand the extent of the effect of interest, we compared the entire distribution in variable v_1 at $p_{\perp 0} = 30\,\text{GeV}$ (right upper plot in fig. 5) with that without one-gauge contribution (bottom plot in fig. 5). Strong interaction in the Higgs sector modifies both one-gauge and two-gauge contributions. The study of charge asymmetry caused by their interference will be a source of information on this strong interaction. One can see that one-gauge contribution is so essential that neglecting it even changes the sign of charge asymmetry (compared to that for the

entire process). Therefore, the charge asymmetry is very sensitive to the interference of two-gauge and one-gauge contributions which is modified under the strong interaction in the Higgs sector. The measurement of this asymmetry will be a source of data on the phase difference of different partial waves of W_LW_L scattering.

3˙5. *If more than one scalar, like Higgs boson, is observed.* It will be a strong argument in favor of more complex Higgs sectors, like 2HDM or something else. It is necessary to measure properties of these scalars, including coupling to fermions, gauge bosons and self-couplings with the best accuracy, to find what model is realized.

To understand properties of the model, one must first measure masses of all scalars and their couplings to gauge bosons and some fermions. However, even these data are non-sufficient for fixing of model parameters. Usually for this goal somebody suggest to measure triple Higgs coupling in the processes like $e^+e^- \to Zhh$, $\gamma\gamma \to hh$. However their cross sections are typically low and contributions of triple Higgs vertexes there are added by contributions of products of other Higgs vertexes. Moreover, knowledge of this vertex is non-sufficient for fixing of model parameters. It was found in [14] the complete set of observable parameters of 2HDM can be extracted from *masses of* $H^\pm$ *and 3 neutrals* h_1, h_2, h_3 (generally with no definite CP parity), *their couplings to gauge bosons*, added by *3 triple Higgs couplings* (like $h_ih_ih_i$ or $H^+H^-h_i$) and *one quartic coupling* (like $H^+H^-H^+H^-$). At high enough energy of PLC the cross sections of processes $\gamma\gamma \to H^+H^-h_i$ are proportional to $\lambda_{H^+H^-h_i}$, unlike to processes with similar final states in another collisions. One can hope also to measure coupling $\lambda_{H^+H^-H^+H^-}$ via measuring of production $\gamma\gamma \to H^+H^-H^+H^-$ cross section.

The information of the complete set of parameters of model will give also information about the way of evolution of phase states of the earlier Universe [15].

4. – New particles

New charged particles will be discovered at LHC and in e^+e^- mode of LC. We expect their decay for final states with invisible particles (like LSP in MSSM).

– How to measure mass, decay modes and spin of these new particles?

In these problems the $\gamma\gamma$ production provides essential advantages compared to e^+e^- collisions.

– How to observe signals from new neutral particles, possible candidates for dark matter?

The cross section of the *pair production* $\gamma\gamma \to P^+P^-$ ($P = S$—scalar, $P = F$—fermion, $P = W$—gauge boson) not far from the threshold is given by QED with reasonable accuracy (see fig. 6).

– These cross sections decrease slowly with energy growth. Therefore, they can be studied relatively far from the threshold where the decay products are almost non-overlapping.

– Near the threshold $f_P \propto (1 + \lambda_1\lambda_2 \pm \ell_1\ell_2 \cos 2\phi)$ with + sign for $P = S$ and − sign for $P = F$. This polarization dependence provides the opportunity to determine the spin of the produced particle P in the experiments with longitudinally polarized photons.

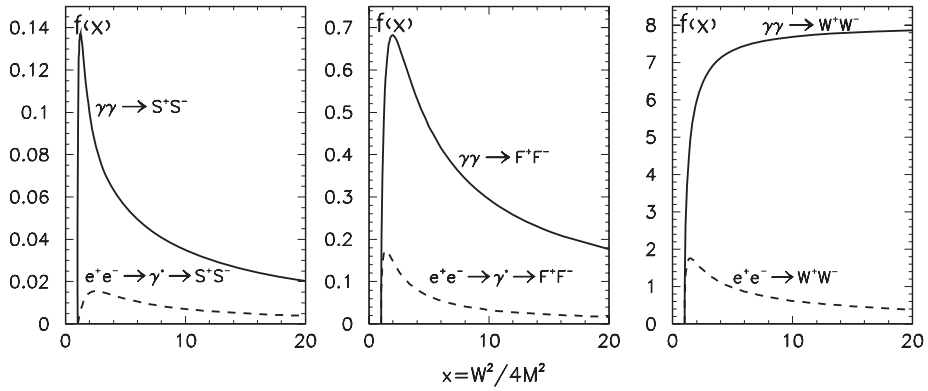

Fig. 6. – $\sigma(\gamma\gamma \to P^+P^-)/(\pi\alpha^2/M_P^2)$, nonpolarized photons, and $\sigma(e^+e^- \to \gamma^* \to P^+P^-)/(\pi\alpha^2/M_P^2)$.

– The polarization of produced fermion or vector P depends on the initial photon helicity. At the P decay this polarization is transformed into the momentum distribution of decay products. *E.g.*, for the SM processes like $\gamma\gamma \to \mu^+\mu^- + neutrals$ (obtained from muon decay modes of $\gamma\gamma \to WW$, $\gamma\gamma \to \tau^+\tau^-$, etc.) muons should exhibit charge asymmetry linked to the polarization of initial photons—see sect. **4**. These studies can help to understand the *nature of candidates for Dark Matter particles*.

The possible CP violation in the $P\gamma$ interaction can be seen as a variation of cross section with changing the sign of both photon helicities (like in fig. 4).

Charge asymmetry in processes $\gamma_\uparrow\gamma_\uparrow \to \mu^+\mu^-\nu_\mu\bar{\nu}_\mu$, $\gamma_\uparrow\gamma_\uparrow \to W^\pm\mu^\mp\nu$. In the SM the effect appears due to P nonconservation in the W-decay.

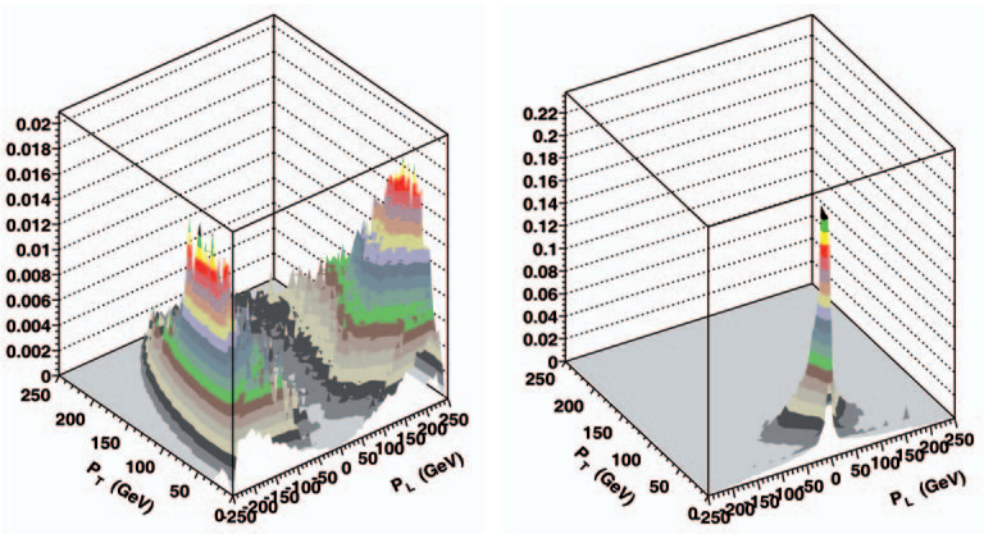

Fig. 7. – Difference between distributions of positive and negative muons for $\gamma_-\gamma_- \to W\mu\nu$.

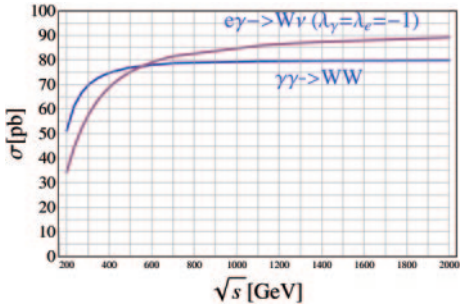

Fig. 8. – Cross sections of 2nd-order processes.

We select events with two cuts, for escape angle θ for each observed particle and for transverse momentum of each observed particle and for missed transverse momentum

$$\pi - \theta_0 > \theta > \theta_0, \qquad p_\perp > p^c_{\perp\mu}. \tag{5}$$

These simultaneous cuts allow to eliminate many backgrounds. We used $\theta_0 = 10\,\text{mrad}$ and study $p^c_{\perp\mu}$ dependence of the effect starting from $p^c_{\perp\mu} = 10\,\text{GeV}$.

Figure 7 demonstrates the charge asymmetry in the collision of two left-polarized photons at $\sqrt{s} = 500\,\text{GeV}$, left and right plots show $p_\perp$, p_L distributions for negative and positive muons, respectively. We find that in the SM the effect is strong and well observable even at large enough $p^c_{\perp\mu} = 100\,\text{GeV}$ [16]. The study of $p^c_{\perp\mu}$ dependence of the effect shows that one can hope to see effects of New Physics in these asymmetries at high transverse momenta (larger than 100 GeV).

5. – Multiple production of SM gauge bosons

The observation of pure interactions of SM gauge bosons (W and Z) or their interaction with leptons will allow to check SM with higher accuracy and observe signals of New Physics. The most ambitious goal is to find deviations from predictions of SM caused by New Physics interactions (and described by anomalies in effective Lagrangian). There are many anomalies relevant to the gauge boson interactions. Each process is sensitive to some group of anomalies. Large variety of processes obtainable at PLC's allows to separate anomalies from each other. The high-energy PLC is the only collider among different future accelerators where one can measure a large number of different processes of such type with high enough accuracy [17].

5˙1. *2nd-order processes.* – The cross sections of basic processes $\gamma\gamma \to W^+W^-$ and $e\gamma \to \nu W$ are so high (fig. 8) that one can expect to obtain about 10^7 events per year providing accuracy better than 0.1%. The cross sections are almost independent of energy and photon polarization [18]. However, final distributions depend on polarization strongly [16].

The accuracy of measurement of these cross sections is sufficient to study in detail 2-loop radiative corrections. Together with standard problems of precise calculations one can note here two non-trivial problems, demanding a detailed theoretical study:

i) *construction of S-matrix for systems with unstable particles*;

ii) *gluon corrections like Pomeron exchange between quark components of W's.*

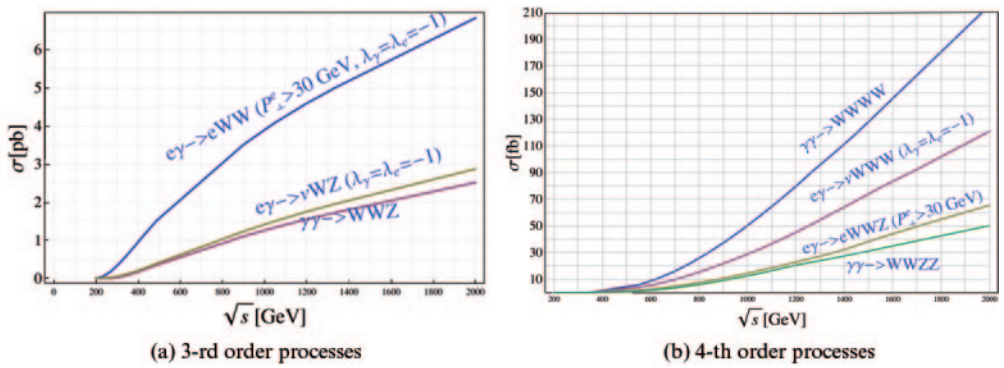

Fig. 9. – Cross sections of 3rd- and 4th-order processes.

The mentioned high values of cross sections of the 2nd-order processes make it possible to measure their multiple "radiative derivatives"—processes of the 3rd- and 4th-order, depending in different ways on various anomalous contributions to the effective Lagrangian.

5˙2. *3rd-order processes*. – We consider here 3 processes (fig. 9a). Total cross section $\sigma_{e\gamma\to eWW} \simeq dn_\gamma \otimes \sigma_{\gamma\gamma\to WW}$. It is very high and easily estimated by equivalent photon method. This large contribution is not very interesting, being only a cross section of $\gamma\gamma \to W^+W^-$ averaged with some weight. However, at large enough transverse momentum of the scattered electron this factorization is violated. Because of it we present $\sigma_{e\gamma\to eWW}$ only for $p_{\perp e} > 30\,\mathrm{GeV}$. Even this small fraction of the total cross section appears so large that it allows *to separate the contribution of* $\gamma Z \to WW$ *subprocess.*

5˙3. *4th-order processes*. – The cross sections of these processes (fig. 9b) are high enough to measure them with 1% precision. For the same reason as for the process $e\gamma \to eWW$ we present the cross section for the process $e\gamma \to eZWW$ only for $p_{\perp e} > 30\,\mathrm{GeV}$. Even this small fraction of the total cross section appears so large that it allows *to separate the contribution of* $\gamma Z \to WWZ$ *subprocess.*

The study of the 2nd-order processes will allow to extract some anomalous parameters or their combinations. The study of the 3rd-order processes will allow to enlarge the number of extracted anomalous parameters and separate some of the combinations extracted from the 2nd-order processes. The study of the 4th-order processes will again enlarge the number of separated anomalous parameters.

6. – Large-angle high-energy photons for exotics

The PLC allows to observe signals from the whole group of exotic models of New Physics in one common experiment. These are models with *large extra dimensions* [19], *point-like monopole* [20], *unparticles* [21]. All these models have a common signature—the cross section for $\gamma\gamma \to \gamma\gamma$ scattering grows with energy as ω^6 ($\omega = \sqrt{s}/2$) and the photons are produced almost isotropically. Future observations either will give limits for scales of these exotics or will allow to see these effects by recording large

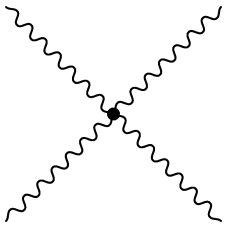

Fig. 10. – Effective Lagrangian.

$p_\perp \sim 0.5$–$0.7E_e$ photons([1]). The study of dependence on the initial photon polarization will be useful to separate the mechanisms.

All these exotics at modern day energies can be described by the effective point-like interaction of fig. 10:

$$L \propto \frac{F^{\mu\nu}F^{\alpha\beta}F_{\rho\sigma}F_{\phi\tau}}{\Lambda^4} \quad (\Lambda^2 \gg s/4). \tag{6}$$

In different models different orders of field indices are realized, Λ is the characteristic mass scale, expressed via parameters of the model. (In all cases s-, t- and u-channels are essential.)

Let us describe the main features of the matrix element (in the photon c.m.s.):

– gauge invariance provides the factor ω for each photon leg;

– to make this factor dimensionless it should be written as ω/Λ. Therefore, the amplitude $\mathcal{M} \propto (\omega/\Lambda)^4 = s^2/(2\Lambda)^4$.

The characteristic scale Λ is large enough not to contradict modern day data. It accumulates other coefficients. The cross section

$$\sigma_{\rm tot} = \frac{1}{32\pi s}\left(\frac{s}{4\Lambda^2}\right)^4, \quad \mathrm{d}\sigma = \sigma_{\rm tot}\Phi\left(\frac{p_\perp^2}{s}\right)\frac{2\mathrm{d}p_\perp^2}{\sqrt{s(s-4p_\perp^2)}} \tag{7}$$

with smooth function $\Phi(p_\perp^2/s)$, describing some composition of S- and D-waves, dependent on the details of the model, and $\int \Phi(z)\frac{2\mathrm{d}z}{\sqrt{1-4z}} = 1$. For large extra dimensions and monopoles the entire s dependence is given by the factor $s^4/(2\Lambda)^8$ from (7), for unparticles the additional factor $(s/4\Lambda^2)^{d_u-2}$ is added.

6˙1. *For the large extra dimensions* case the point in fig. 10 describes an elementary interaction, given by the product of stress-energy tensors T_{ab} for the incident and the final photons, that are exchanging the tower of Kaluza-Klein excitations (with permutations), *i.e.* $\mathcal{M}_{\gamma\gamma\to\gamma\gamma} \propto \langle T_{ab}T^{ab}/\Lambda^4\rangle \approx F^{\mu\nu}F_{\nu\alpha}F^{\alpha\beta}F_{\beta\mu}/\Lambda^4 + \textit{permutations}$. After averaging over polarizations for tensorial KK excitations

$$\Phi \propto 2(1-p_\perp^2/s)^2 = (3+\cos^2\theta)^2/8 = (\hat{s}^4+\hat{t}^4+\hat{u}^4)/2\hat{s}^4. \tag{8}$$

([1]) In my personal opinion it is hardly probable that these models describe reality.

Unlike ILC1, at high-energy PLC the other channels (like $\gamma\gamma \to WW$) are less sensitive to the extra-dimension effect.

6˙2. *The point-like Dirac monopole* existence would explain the mysterious quantization of an electric charge since in this case $ge = 2\pi n$ with $n = 1, 2, \ldots$. *There is no place for this monopole in modern theories of our world but there are no precise reasons against its existence.* In this case the point in fig. 10 corresponds to exchange of loop of heavy monopoles (like electron loop in QED—Heisenberg-Euler-type Lagrangian).

Let M be a monopole mass. At $s \ll M^2$ the electrodynamics of monopoles is expected to be similar to the standard QED with the effective perturbation parameter $g\sqrt{s}/(4\pi M)$ [20]. The $\gamma\gamma \to \gamma\gamma$ scattering is described by a monopole loop, and it is calculated within QED,

$$\mathcal{L}_{4\gamma} = \frac{1}{36}\left(\frac{g}{\sqrt{4\pi}M}\right)^4 \left[\frac{\beta_+ + \beta_-}{2}(F^{\mu\nu}F_{\mu\nu})^2 + \frac{\beta_+ - \beta_-}{2}\left(F^{\mu\nu}\tilde{F}_{\mu\nu}\right)^2\right].$$

The coefficients $\beta_\pm$ and details of angular and polarization dependence depend strongly on the spin of the monopole.

After averaging over polarizations, the $p_\perp$ dependence and the total cross section are described by the same equations as for the extra dimensions case. The parameter Λ is expressed via the monopole mass and the coefficient a_J, dependent on the monopole spin J ($n = 1, 2, \ldots$):

$$\Lambda = (M/n)a_J, \qquad \text{where} \qquad a_0 = 0.177, \quad a_{1/2} = 0.125, \quad a_1 = 0.069. \tag{9}$$

6˙3. *Unparticle* $\mathcal{U}$ is an object, describing particle scattering via a propagator which has no poles at the real axis. It was introduced in 2007 [21]. This propagator behaves (in the scalar case) as $(-p^2)^{d_U-2}$ where the scalar dimension d_u is not integer or half-integer. The interaction carried by the unparticle is described as $\frac{F^{\mu\nu}F_{\mu\nu}\mathcal{U}}{\Lambda^{2d_U}}$ with some phase factor. For matrix element it gives

$$\mathcal{M} = \frac{F^{\mu\nu}F_{\mu\nu}F^{\rho\tau}F_{\rho\tau}}{\Lambda^{4d_U}}(-P^2)^{d_U-2} + \text{permutations}, \tag{10}$$

$$|\mathcal{M}|^2 = C\frac{s^{2d_U} + |t|^{2d_U} + |u|^{2d_U} + \cos(d_u\pi)\left[(s|t|)^{d_U} + (s|u)^{d_U}\right] + (tu)^{d_U}}{\Lambda^{4d_U}}.$$

6˙4. *The anticipated discovery limits* for all these models are shown in table II. The results of D0 experiment [22], recalculated to used notations, are also included here. For the unparticle model presented numbers are modified by corrections $\propto (d_U - 2)$.

TABLE II. – *The obtainable discovery limits.*

	Λ	Reference
Tevatron D0	175 GeV	[22]
LHC	2 TeV	[20]
$\gamma\gamma$ ($100\,\mathrm{fb}^{-1}$)	$3E_e$	[20]
e^+e^- LC ($1000\,\mathrm{fb}^{-1}$)	$2E_e$	[20]

* * *

This paper is supported by grants RFBR 08-02-00334-a, NSh-3810.2010.2, Program of Dept. of Phys. Sc RAS "Experimental and theoretical studies of fundamental interactions related to LHC" and INFN grant.

REFERENCES

[1] GINZBURG I. F., KOTKIN G. L., SERBO V. G. and TELNOV V. I., *Nucl. Instrum. Methods*, **205** (1983) 47; GINZBURG I. F., KOTKIN G. L., PANFIL S. L., SERBO V. G. and TELNOV V. I., *Nucl. Instrum. Methods*, **219** (1983) 5.
[2] BADELEK B. *et al.*, *TESLA TDR*, hep-ex/0108012.
[3] TELNOV V., hep-ex/0012047.
[4] GINZBURG I. F., KOTKIN G. L. and SERBO V. G., in preparation.
[5] WITTEN E., *Nucl. Phys. B*, **120** (1977) 189.
[6] JIKIA G. and SÖLDNER-REMBOLD S., *Nucl. Phys. B (Proc. Suppl.)*, **82** (2000) 373; MELLES M., STIRLING W. J. and KHOZE V. A., *Phys. Rev. D*, **61** (2000) 054015.
[7] GINZBURG I. F., KRAWCZYK M. and OSLAND P., *Nucl. Instrum. Methods A*, **472** (2001) 149; hep-ph/0101229.
[8] GINZBURG I. F. and IVANOV I. P., *Eur. Phys. J. C*, **22** (2001) 411.
[9] CHERNYAK V. L. and SERBO V. G., *Nucl. Phys. B*, **67** (1973) 464; GINZBURG I. F., SCHILLER A. and SERBO V. G., *Eur. Phys. J. C*, **18** (2001) 731.
[10] GINZBURG I. F., *Proc. 9th Int. Workshop on Photon-Photon Collisions, San Diego (1992)*, p. 474.
[11] GINZBURG I. F. and KANISHEV K. A., hep-ph/0507336.
[12] PUKHOV A., hep-ph/0412191.
[13] GINZBURG I. F. and SERBO V. G., *Phys. Lett. B*, **96** (1980) 68.
[14] KANISHEV K. A., in preparation.
[15] GINZBURG I. F., IVANOV I. P. and KANISHEV K. A., hep-ph/0911.2383.
[16] ANIPKO D. A., GINZBURG I. F., KANISHEV K. A., PAK A. V., CANNONI M. and PANELLA O., *Phys. Rev. D*, **78** (2008) 093009; ArXive: hep-ph/0806.1760.
[17] GINZBURG I. F., ILYIN V. A., PUKHOV A. E., SERBO V. G. and SHICHANIN S. A., *Phys. At. Nucl.– Russ. Yad Fiz.*, **56** (1993) 57.
[18] GINZBURG I. F., KOTKIN G. L., PANFIL S. L. and SERBO V. G., *Nucl. Phys. B*, **228** (1983) 285.
[19] DIENES K. R., DUDAS E. and GHERGHETTA T., hep-ph/9803466, *Phys. Lett. B*, **436** (1998); SHIFMAN M., hep-ph/09073074.
[20] GINZBURG I. F. and PANFIL S. L., *Sov. Yad. Fiz.*, **36** (1982) 850; GINZBURG I. F. and SCHILLER A., *Phys. Rev. D*, **60** (1999) 075016.
[21] GEORGY H., *Phys. Rev. Let.*, **98** (2007) 221601; hep-ph/0703.260; SAHIN I. and INAN S. C., hep-ph/09073290.
[22] ABBOT B. *et al.*, *Phys. Rev. Lett.*, **81** (1998) 524, hep-ex/9803023.